Proc. Nat. Acad. Sci. USA
Vol. 71, No. 7, pp. 2818–2822, July 1974

The Density of Acetylcholine Receptors and Their Sensitivity in the Postsynaptic Membrane of Muscle Endplates

(bat/binding sites/α-bungarotoxin/ionic conductance modulator/skeletal muscle/vertebrates)

EDSON X. ALBUQUERQUE*†, ERIC A. BARNARD‡§, CARL W. PORTER‡, AND JORDAN E. WARNICK§

Departments of * Pharmacology, ‡ Biochemistry, and § Biochemical Pharmacology, State University of New York at Buffalo, Buffalo, N.Y. 14214

Communicated by Bernhard Witkop, April 23, 1974

ABSTRACT **In various skeletal muscles, the *mean* density of acetylcholine receptors in the muscle postsynaptic membrane is constant at about 8700 per μm^2, even though the overall size of an endplate ranged from 400 μm^2 to 1300 μm^2 in these muscles. This measurement was by electron microscope autoradiography of α-[^{3}H]bungarotoxin binding sites; only one-half of these, however, appear to be true active centers of the acetylcholine receptor. The highest density of these receptors is on the juxtaneuronal regions of the postsynaptic membrane, and their density in the depths of the fold is less than one quarter of that at the tips. A maximum sensitivity to externally applied acetylcholine, about 3000–5000 mV/nC, is found in diverse types of endplates when truly focal recording is achieved. This acetylcholine sensitivity appears to be determined by the local density of receptors in the membrane, and not by their total number at the endplate. A quantal efficiency term is also disclosed. The maximal sensitivity per molecule obtainable by microiontophoresis of acetylcholine is 5–10% of that operative when a quantum reacts. When acetylcholine is released from a vesicle, in contrast to its application from outside, geometric factors are more favorable. Consideration of the local packing density, acetylcholine molecule numbers, and the current flow when one quantum of acetylcholine interacts at the membrane suggests that one, or possibly two, activated receptor active centers are linked to one open gate of the ionic conductance modulator.**

At the motor endplate of vertebrate skeletal muscles acetylcholine (AcCh) is known to bind specifically to receptor molecules, which logically should be in the postsynaptic membrane (1–3). The only direct determination of receptor distribution at the endplate (4, 5) and for the electroplaque (6), has been by autoradiography in the electron microscope of tissues treated with a radioactive α-neurotoxin, such as α-bungarotoxin (BuTX), which reacts specifically and essentially irreversibly with cholinergic nicotinic receptors (7–10). Thus, an average density of 8500 AcCh receptor active centers per μm^2 of postsynaptic membrane has been determined for mouse diaphragm endplates (5).

A knowledge of the AcCh receptor density at the muscle endplate region is needed for interpretation of the true level of AcCh sensitivity, i.e., the membrane depolarization evoked by the reaction of a given quantity of released AcCh. Such sensitivity at the nicotinic receptor/membrane system has been estimated experimentally by microiontophoretic application of AcCh at the endplate region of innervated skeletal muscle, and also at extra-junctional regions of denervated muscle, where marked responsiveness to AcCh develops (11–15). It is, however, extremely difficult to locate precisely the endplate with the conventional stereomicroscope used in the latter type of study. In contrast to the 300–800 mV/nC range of junctional AcCh sensitivities previously reported, we shall show that much larger values, of the order of 2500–5000 mV/nC, can be obtained at vertebrate motor endplates when a Nomarski optical system is used, or in rare fortunate encounters among a very large number of recordings with the conventional stereomicroscope technique.

The questions which we shall consider here are: (*i*) What is the maximum AcCh sensitivity obtainable by microiontophoretic application of AcCh at the endplate, and how comparable is this AcCh sensitivity with the intrinsic sensitivity of the postsynaptic membrane to endogenous AcCh? (*ii*) Is the AcCh sensitivity of the postsynaptic membrane determined by the total number or by the density of AcCh receptors? (*iii*) Is the surface density of the AcCh receptors a constant value in different vertebrate muscle endplates? (*iv*) Are the AcCh receptors uniformly dispersed along the postsynaptic membrane? (*v*) How does the total number of AcCh receptors per endplate vary at different endplate types in different animal species.

MATERIALS AND METHODS

Male albino mice (RR strain; weight 19–22 g), chickens 12–16 weeks *ex ovo* (New Hampshire normal strain 200, from the University of California at Davis flock) and an American brown bat, *Eptisicus fuscus* (weight 14 g), were used.

Electrophysiological Recordings. The mouse sternomastoid or left diaphragm muscles were excised with attached nerves; frog (*Rana pipiens*) cutaneous pectoral muscles (17) were also taken. For studies without Nomarski optics, the muscles were prepared as described elsewhere (10, 15). The preparations were kept at room temperature (22–23°) in the appropriate Krebs–Ringer (Ringer) solution aerated with 95% O_2–5% CO_2. For studies with Nomarski optics, the sternomastoid, diaphragm, and cutaneous pectoral muscles were dissected to leave only a few layers of intact fibers. The position of the microelectrode was considered focal when the rise time of the

Abbreviations: AcCh, acetylcholine; BuTX, α-bungarotoxin; DFP, diisopropyl fluorophosphate.

† To whom reprint requests should be addressed at Department of Cell Biology and Pharmacology, University of Maryland School of Medicine, Baltimore, Md. 21201.

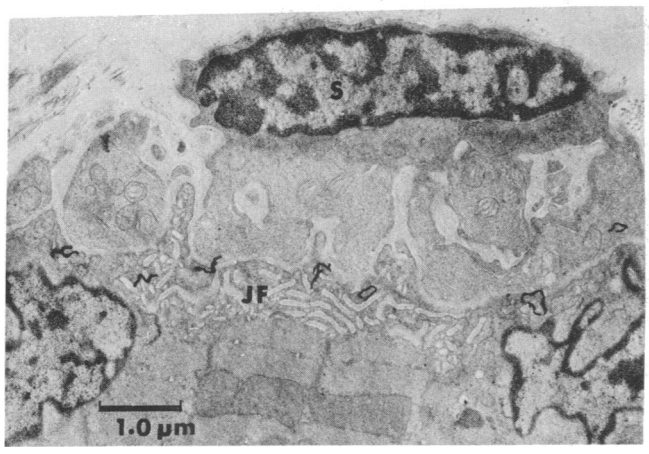

FIG. 1. Autoradiograph of a portion of a bat diaphragm endplate labeled with [^{3}H]BuTX. Typically, the grains lie over the postjunctional folds (*JF*) or within the range of radiation scatter from them. The axon and Schwann cell (*S*), and the rest of the muscle cell, are always negligibly labeled in comparison with the folds and cleft.

spontaneous miniature endplate potentials was < 0.7 msec. In the sternomastoid muscle, only the "fast" white fibers of the muscle were selected. The micropipettes filled with 2 M AcCh had resistances of 350–600 MΩ.

To assess the accuracy of our studies with mammalian muscles, we first compared the AcCh sensitivity of the frog muscle using these two techniques (Nomarksi and conventional stereoscopic optics): we obtained results similar to those of Peper and McMahan (16), i.e., an AcCh sensitivity as high as 2533 mV/nC with a rise time for the potential of 2.1 msec.

TABLE 1. *Molecular parameters of various neuromuscular junctions*

Muscle	Mean diameter of fibers (μm)	Total number of receptor sites*† (millions)	Density (number of receptors*/ μm² of post-synaptic membrane)	Maximum AcCh sensitivity (mV/nC)‡
Mouse diaphragm	21	31	8500	2862
Mouse sternomastoid (white)	40	87	8800	3619
Bat diaphragm	18		8800	
Chicken posterior latissimus dorsi	35	36		2800§
Frog cutaneous pectoris	48			2533
Frog sartorius	60	30		

* Taken as all of the [^{3}H]BuTX-binding sites.

† Obtained using the total numbers of DFP-reactive sites per endplate (19) for these fibers, and the BuTX/DFP-reactive sites ratio of 1.0 (4, 7) for these muscles.

‡ Mean of all values higher than 2000 mV/nC. (The highest value for the diaphragm was on a fiber of 26-μm diameter, and that for the sternomastoid, 43-μm.)

§ See ref. 40.

Labeling, Electron Microscope Autoradiography, and Morphometric Studies. Pure BuTX and its [^{3}H]acetylated derivative, prepared as described (9), were injected intravenously into animals at a supralethal dose (3 μg/g of body weight). The muscle was washed, processed, sectioned at 100 nm, and coated with a monolayer of Ilford L-4 emulsion (5). The diameters of the muscle fibers whose AcCh sensitivity is shown in Figs. 3 and 4 were obtained after sectioning of frozen muscles. The identification of these fibers was made with the aid of a dye marker as described elsewhere (20). After staining of the muscles for cholinesterase (21), the overall surface area of the motor endplate and muscle fiber diameter were measured on photographic prints of stained, isolated fibers, as described by Kuno *et al.* (22) except that these muscles were fixed in 4% neutral formaldehyde, 16 hr, 4°.

RESULTS AND DISCUSSION

Receptor Density at Postsynaptic Membranes. The techniques of electron microscope autoradiography, used in the previous study (5) of receptor distribution at mouse diaphragm endplates, were applied to the diaphragm muscle of another mammal phylogenetically quite distant from the mouse, namely, the American brown bat. The developed grains in the electron microscope autoradiographs were found to be associated (to the extent of 95% of all of the grains found) with the synaptic membranes and cleft (Fig. 1). Their actual distribution was as found for the mouse diaphragm (5), and fits the theoretical curve (23) for the scatter of radiation from a radioactive line source at the postsynaptic membrane. The total number of grains associated thus with the postsynaptic membrane in the section was as 310, and the total length of the postjunctional membrane measurable in the same sections was 1700 μm. From the known (interferometrically-monitored) section thickness, the total surface area of these membrane regions was at once derived. The absolute number of [^{3}H]BuTX molecules present was obtained from the specific activity (4.1 Ci/mmole) of the reagent, the emulsion exposure period, and the sensitivity of the emulsion batch used (5). An average density of 8800 binding sites per μm² of postsynaptic membrane was obtained thus for the diaphragm muscle of the bat, a value similar to that obtained for the mouse diaphragm endplate (Table 1, column 4).

An estimation can also be made of the corresponding mean density at another type of endplate, in fast fibers of the mouse sternomastoid. The membrane density of the reaction sites of [^{3}H]diisopropyl fluorophosphate (DFP) there has recently been measured by electron microscope autoradiography (23). From autoradiographic analysis we also know the ratio of [^{3}H]DFP-reactive sites to [^{3}H]BuTX-binding sites at this same endplate (Table 1) is about 1.0. Hence, assuming that the [^{3}H]-BuTX sites are again located on the postsynaptic membrane, their density is as for the other two endplate types (Table 1). In all the mammalian muscle types thus far examined, the value for the AcCh receptor density (averaged over the entire postsynaptic membrane at the endplate) appears to be constant.

The *local* density in those regions of the postsynaptic membrane closest to the axon, however, is significantly higher

than the mean value cited. When a histogram is plotted of the grains lying over junctional folds of membranes of mouse diaphragm endplates against the distances from their axonal membranes (Fig. 2*A*), the grains are seen to be concentrated in the zones nearest to the axon. This effect was seen in the previous study on mouse diaphragm (see Fig. 4 of ref. 5) but was not then regarded as evidence of such nonuniformity because of the small amount of the sample in the distal zone. However, when more such [^{3}H]BuTX-labeled diaphragm was processed and larger numbers of grains counted, the effect became significant (Fig. 2*A*). The density over the first two bin columns, contributed by grains over unfolded membrane at the top one-third of the folds, is at least four times that over the last bins, contributed largely by grains over membrane at the bottom half of the folds. We cannot specify from this histogram the form of the gradient down the fold, due to the resolution limit, but the asymmetry is clear, and is not seen at all in similar plots from [^{3}H]DFP-labeled material. The density near the tops of the folds and in the unfolded postsynaptic membrane is estimated to be about 18,000 BuTX sites per μm^2. Evidence to support this interpretation of receptor distribution comes from recent reports on freeze-etched preparations from endplates in various muscles (24, 25). Characteristic 100 to 140-Å particles, which were presumed to include receptor–ionic conductance modulator complexes, were observed on the postsynaptic membrane, and were more concentrated on the juxta-neuronal portions of the folds, their density there (about 2500 per μm^2) being roughly four times that deep in the folds. This correspondence suggests that these particles carry the BuTX-binding sites (and gives the tentative value of 6 of these per particle).

Acetylcholine Sensitivity at Endplates of Mouse Muscles. The AcCh sensitivity observed at the endplate of the diaphragm fibers of the mouse (n = 6 animals), using a conventional dissecting stereomicroscope (see *Materials and Methods*), ranged from 275 to 2239 mV/nC (Fig. 3*A*), and for white fibers of the sternomastoid muscles from 180 to 2314 mV/nC (Fig. 3*B*). The highest sensitivities were on a fiber of 22-μm diameter (diaphragm) and 43-μm (sternomastoid). A total of 600 surface fibers was investigated with the stereomicroscope in six diaphragm and six sternomastoid muscles, and only on three or four occasions were values > 2000 mV/nC obtained. The smallest rise time of the AcCh potential of the surface fibers of the diaphragm muscles was 2.18 msec and for the sternomastoid muscles was 2.59 msec. Locating high AcCh sensitivity regions was much easier with visualization of endplates by Nomarski optics (Fig. 4), so that 26 of the 200 sternomastoid fibers studied in six muscles then showed values in the range 2010–4730 mV/nC (Table 1). For the smaller fibers present in the mouse diaphragm, location was much more difficult, and only four fibers out of 80 showed AcCh sensitivity > 2000 mV/nC (Fig. 4, Table 1). The smallest rise time of the AcCh potential obtained in fibers of diaphragm or sternomastoid muscles was 1.60 msec (amplitude of the AcCh potential = 5.01 mV) or 1.86 msec (amplitude = 8.62 mV), respectively. Even though the fibers of the diaphragm have smaller diameters than those of the sternomastoid (see below) and endplate regions three to four times smaller, the AcCh sensitivities among the various endplates of both muscles were roughly similar.

Sizes of Fibers and Endplates. The overall area occupied by the endplate region on the fibers of six sternomastoid muscles

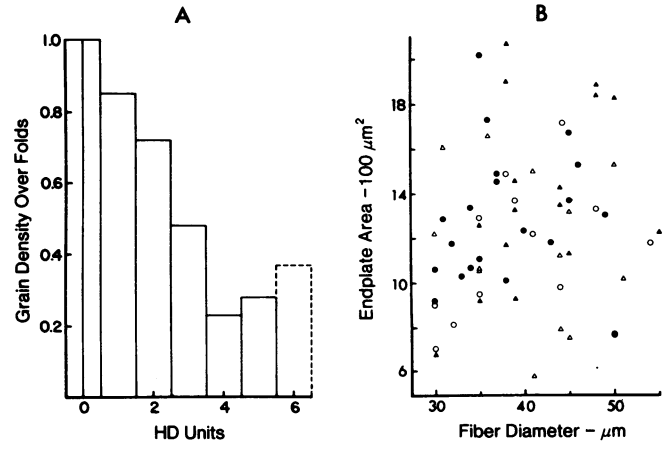

FIG. 2. (*A*) Histogram of grain densities over the postjunctional folds of mouse diaphragm. The area determinations, to obtain these densities, were made using a uniform grid of points. Only points and grains that lay over the folds were considered. A total of 510 grains and 1400 grid points were used. Distances, in half-distance (*HD*) units [a unit of resolution (23)], are measured here with the *axonal membrane* as origin. The *broken line* indicates a region where estimates are unreliable, since only 2% of the total grains were found there. (*B*) Relationship between overall endplate area and fiber diameter of the fast fibers of the sternomastoid muscle. The various symbols indicate the individual endplates obtained from fibers of four muscles. The mean endplate area was 1255 ± 347 μm^2 (± SD); the mean fiber diameter was 39.9 ± 6.7 μm. Correlation coefficient = 0.17.

(see Fig. 2*B*) was 1255 ± 347 μm^2 (± SD) and the mean fiber diameter was 39.9 ± 6.7 μm. For four diaphragm muscles, the mean endplate area of 90 fibers was 392 ± 110 μm^2, and fiber diameter was 20.7 ± 4.2 μm. A plot of muscle fiber diameter versus endplate area revealed a positive correlation which was highly significant in the diaphragm muscle ($P < 0.001$), but *not* significant ($P > 0.5$) in the sternomastoid muscle (Fig. 2*B*).

Total Numbers of Receptor Sites at the Endplate in Various Muscles. While the membrane density of [^{3}H]BuTX-binding sites is constant in the endplates studied (Table 1), the total number of such sites at the endplate (= density × postsynaptic surface area) varies considerably between muscle fiber types. These total numbers are obtained (7) by use of the [^{32}P]DFP reaction (with cholinesterase-type active centers) at the endplate, which has been quantitated in

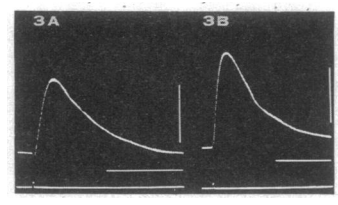

FIG. 3. AcCh potentials at the endplate region of the surface fibers of diaphragm muscle (*A*) and "white" surface fibers of the sternomastoid muscle (*B*) of the mouse, visualized by conventional stereomicroscope optics. Current pulses are 0.3 msec (*A*) and 0.5 msec (*B*). Total charge, 2.7 pC (*A*) or 5.4 pC (*B*). *Vertical bar* = 5 mV (*A*) or 7.5 mV (*B*); *horizontal bar* = 10 msec.

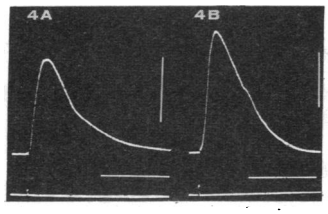

FIG. 4. AcCh potentials at the endplate region from the diaphragm muscle (*A*) and "white" surface fibers of the sternomastoid muscle (*B*) of the mouse, visualized by Nomarski optics. Total charge, 3.0 pC (*A*) or 4.28 pC (*B*). *Vertical bar* = 5 mV; *horizontal bar* = 10 msec; current pulses, 0.3 msec.

absolute terms by β-track counting (26). This provides an internal standard for each endplate, irrespective of the identity of the sites reacting with DFP. The ratio of [^{3}H]DFP-reactive sites to [^{3}H]BuTX-binding sites at these endplate types has been found to be 1.0 in each case (4, 7), so that the absolute number of DFP-reactive sites at that type of endplate (19) immediately discloses the number of BuTX-binding sites there (Table 1, column 3). This comparative method does not rely upon the assumption that the DFP-reactive and BuTX-binding sites are at the same location, since only the overall number per endplate is involved in each case. In fact, however, the topography of the [^{3}H]-BuTX-binding sites (Fig. 2*A*) is rather different from that (23) of the [^{3}H]DFP-reactive sites, the latter being spread more widely over the folds and cleft than the former.

It has been shown in mammalian muscles that binding of [^{3}H]BuTX at the endplate occurs at two types of sites (9, 10, 27). One-half of the binding sites have the properties of the AcCh receptor, having a high affinity for *d*-tubocurarine and losing all response to AcCh upon treatment with BuTX. The other half do not have the properties just cited, and are thought likely to be on the ionic conductance modulator component of the receptor system (9, 28, 29). The numbers of [^{3}H]BuTX-binding sites listed in Table 1 should probably, then, be divided by 2 to give the numbers of AcCh-binding receptor active centers. Since more information on the receptor–ionic conductance modulator complex is not available, we have listed the total numbers of [^{3}H]BuTX-binding sites as functional receptor centers, with the reservation, however, that these may comprise two different types.

Relationships Between Membrane Receptor Density, Receptor Number, and Acetylcholine Sensitivity. We can now consider the questions posed in the introductory section. Questions (*iii*) and (*v*) are answered, for the samples available to date, in Table 1. Some evidence on question (*iv*) is supplied by the distribution of [^{3}H]BuTX sites discussed above. We turn now to questions (*i*) and (*ii*). The maximal obtainable response at the endplate to applied AcCh is apparently approached by the values reported here (Table 1, column 5), because the rise time of the potential in those cases was < 1.5 times that of the endplate potential. This maximally attainable AcCh sensitivity is essentially the same in the four diverse endplate types tested (Table 1). Although the total number of receptors (the mean per endplate) varies considerably among those various endplate types, the mean membrane density of these receptors is constant (Table 1). The total number of receptors increases with the diameter of the fiber in a given muscle type (5, 19), but the high values of AcCh sensitivity obtained were seen indiscriminately on both large and small fibers. We conclude that AcCh sensitivity is determined by the local density of the receptors and not by their total population at the endplate. This seems reasonable, since a radial front of AcCh flux that is small compared to the overall dimensions (Fig. 2*B*) of the endplate must give rise to the maximum potentials registered; the short rise time indicates that the pipette is then a very few μm from the postsynaptic membrane. Hence, the probability of collisions of AcCh molecules with receptors during the rise time is obviously determined by the local density of receptors that is encountered, and the AcCh concentration is presumed to be depleted rapidly by receptor binding (compare ref. 30). The same should occur with natural quanta.

Cholinergic nerve endings that release very small numbers of quanta per impulse (e.g., 1–15 quanta in spinal motoneurons) have very much smaller terminal areas, suggesting that the area of the postsynaptic membrane is adapted to the number of quanta needed for synaptic function. This would be the case if the average surface density of AcCh receptors is always constant, as in all the neuromuscular junctions investigated thus far. There is no necessity, however, for the postsynaptic membrane area to be correlated in a simple manner with the gross projected area of the endplate. The latter has been correlated with the muscle fiber diameter (22), but with a considerable amount of scatter; there is no correlation in the mouse sternomastoid (Fig. 2*B*). The anatomical details of the insertion of the nerve endings on the muscle vary between red and white fiber types, and between species, so that the gross projected area of the endplate need not show a simple relationship to the other parameters considered here.

For comparison, we can estimate the value of the sensitivity to AcCh released neurally. About 1.5×10^4 molecules of AcCh are released for a miniature endplate potential of 0.5 mV, at the endplate of the rat diaphragm muscle at 20° (31). With an AcCh micropipette of the size we have used, a calibration (18) with [^{3}H]AcCh (but using charges > 2 μC) has shown that roughly 2×10^9 molecules of AcCh are actually released per nC of charge passed. Hence, there is an intrinsic sensitivity of about 50,000–60,000 mV/nC for AcCh packets of quantal size. The difference between this latter intrinsic sensitivity and that of about 4000 mV/nC to externally applied AcCh means that a quantal efficiency of only about 8% is attained in the latter case, a value which may need a small upward correction, since for the very small charges used here, the current loss will give a proportionately greater error than in the calibration experiments, where it was negligible (18). The results suggest, therefore, that roughly 90% of the AcCh molecules escape elsewhere into the medium even during the most efficient release from the micropipette directly over the endplate.

We must note here (*i*) that the maximum value for the microiontophoretic AcCh sensitivity reached a limit that was not exceeded as the pipette was placed nearer to the endplate, even when the rise time of the potential was of the same order as that of the miniature endplate potential rise time; (*ii*) the latency was < 120 μsec, this being of the same order of magnitude as the calculated maximum diffusion time for neurally released transmitter in the cleft (1, 32); (*iii*) Peper and McMahan (16) have reported that removal of the nerve terminal from a frog endplate, which exposes a large area of postsynaptic membrane, does not increase the sensitivity or decrease the rise time of an AcCh potential. Diffusion barriers to externally applied AcCh can, of course, often be present

over the endplate. The limited external opening of the cleft, or an obstruction by a Schwann cell (16), can account for the many low values recorded focally, but when the maximum sensitivity is recorded we conclude that fortunate positioning has probably avoided such obstacles. In these cases, then, the the only geometric contribution to the large inefficiency noted can be the escape of the AcCh molecules that are not in that sector of the radial diffusion wave that impinges on the endplate. Estimates of this effect have been given by others (33, 34), and since, in our case, the source radius is of the same order as, or smaller than, the diameter of the sensitive area affected, it is uncertain whether or not this geometric factor would account for the entire loss of about 90% in efficiency. The possibility that there is some contribution by an additional component that renders receptor activation by AcCh of vesicular origin more efficient cannot be excluded at this time.

Relationship of AcCh Receptors to Ionic Conductance Modulator Sites. On a simple diffusion model, the AcCh molecules in a single quantal packet when released into the cleft should reach a concentration of about 10 μM at 1-μm radius from the origin in 0.3 msec (32). Since this interval is the rise time of the unit miniature endplate current (33, 35, 36), we define thus the zone of effectiveness of one quantum, at least as a minimum. This is a patch of about 3 μm^2 of postsynaptic membrane. The maximum effect produced there is a conductance change of about 2×10^{-7} mho, as estimated (35) for one miniature endplate current in the frog sartorius endplate. The most recent estimate of the minimum conductance for such an endplate per open ion channel is 3×10^{-11} mho (37). Hence, a maximum of about 6000 single channels should be open for the generation of one miniature endplate current. The membrane patch involved would have a high probability of being in the zone closer to the axon, and would, taking the values above [and the observed asymmetry (Fig. 2*A*)], contain at least 30,000 true functional centers of the AcCh receptor (i.e., 60,000 BuTX-binding sites). Only 10,000–20,000 AcCh molecules are released; some of these are lost by prior hydrolysis and not more than 70% of those surviving become, according to the recent evidence of Katz and Miledi (38), receptor-bound. These available receptor sites, therefore, *cannot be saturated by the transmitter.* Nevertheless, recent data on the AcCh receptor blockade/response relationship at the endplate (39) show that only about 25% of the entire number of functional receptor centers can be removed without diminishing the response to neurally-released AcCh. Since about 6000 channels are opened, these values indicate that there are one, or at the most two, AcCh-activated receptor sites per available ion channel.

This work was supported by U.S. Public Health Service Grants NS-08233 and GM-11754. C.W.P. was a pre-doctoral trainee supported by a training grant in Pathology from the National Institutes of General Medical Sciences, 01-1500.

1. Eccles, J. C. (1964) *The Physiology of Synapses* (Springer-Verlag, Heidelberg, Germany).
2. Hubbard, J. I. (1973) *Physiol. Rev.* **53,** 674–723.
3. Eccles, J. C. & Jaeger, J. C. (1957) *Proc. Roy. Soc. Ser. B* **148,** 28–56.
4. Porter C. W., Chiu, T. H., Wieckowski, J. & Barnard, E. A. (1973) *Nature New Biol.* **241,** 3–7.
5. Porter, C. W., Barnard, E. A. & Chiu, T. H. (1973) *J. Membrane Biol.* **14,** 383-402.
6. Bourgeois, J.-P., Ryter, A., Menez, A., Fromageot, P., Boquet, P. & Changeux, J.-P. (1972) *FEBS Lett.* **25,** 127–133.
7. Barnard, E. A., Wieckowski, J. & Chiu, T. H. (1971) *Nature* **234,** 207–211.
8. Lee, C. Y. (1972) *Ann. Rev. Pharmacol.* **12,** 265–286.
9. Albuquerque, E. X., Barnard, E. A., Chiu, T. H., Lapa, A. J., Dolly, J. O., Jansson, S.-E., Daly, J. & Witkop, B. (1973) *Proc. Nat. Acad. Sci. USA* **70,** 949–953.
10. Lapa, A. J., Albuquerque, E. X. & Daly, J. (1974) *Exp. Neurol.* **43,** 375–398.
11. Albuquerque, E. X. & McIsaac, R. J. (1970) *Exp. Neurol.* **26,** 183–202.
12. Axelsson, J. & Thesleff, S. (1959) *J. Physiol. (London)* **147** 178–193.
13. Krnjevic, K. & Miledi, R. (1958) *Nature* **182,** 805–806.
14. Kuffler, S. W. (1943) *J. Neurophysiol.* **6,** 99–110.
15. McArdle, J. J. & Albuquerque, E. X. (1973) *J. Gen. Physiol.* **61,** 1–23.
16. Peper, K. & McMahan, U. J. (1972) *Proc. Roy. Soc. Ser. B* **181,** 431–440.
17. Braun, M. & Schmidt, R. F. (1966) *Pflügers Arch. Gesamte Physiol. Menschen Tiere* **287,** 56–80.
18. Bradley, P. B. & Candy, J. M. (1970) *Brit. J. Pharmacol.* **40,** 194–201.
19. Barnard, E. A., Chiu, T. H., Jedrzejcyzk, J., Porter, C. W. & Wieckowski, J. (1973) in *Drug Receptors,* ed. Rang, H. P. (McMillan, London), pp. 225–240.
20. Wilson, V. J., Kato, M., Thomas, R. C. & Peterson, B. W. (1966) *J. Neurophysiol.* **29,** 508–529.
21. Koelle, G. B. & Friedenwald, J. S. (1949) *Proc. Soc. Exp. Biol. Med.* **70,** 617–622.
22. Kuno, M., Turkanis, S. A. & Weakly, J. N. (1971) *J. Physiol. (London)* **213,** 545–556.
23. Salpeter, M. M., Plattner, H. & Rogers, A. W. (1972) *J. Histochem. Cytochem.* **20,** 1059–1068.
24. Rash, J. E., Ellisman, M. H., Staehelin, L. A. & Porter, K. R. (1974) *Proc. Int. Conf. of the Muscular Dystrophy Assoc. of America,* October 14–19, 1973, *Excerpta Medica,* in press.
25. Heuser, J. E., Reese, T. S. & Landis, D. M. D. (1974) *J. Neurocytol.* **3,** 109–131.
26. Rogers, A. W., Darzynkiewicz, A., Salpeter, M. M., Ostrowski, K. & Barnard, E. A. (1969) *J. Cell Biol.* **41,** 665–685.
27. Chiu, T. H., Lapa, A. J., Barnard, E. A. & Albuquerque, E. X. (1974) *Exp. Neurol.* **43,** 399–413.
28. Kuba, K., Albuquerque, E. X., Daly, J. & Barnard, E. A. (1974) *J. Pharmacol. Exp. Ther.* **189,** 499–512.
29. Albuquerque, E. X., Kuba, K., Lapa, A. J., Daly, J. & Witkop, B. (1974) *Proc. Int. Conf. of the Muscular Dystrophy Assoc. of America,* October 14–19, 1973, *Excerpta Medica,* in press.
30. Katz, B. & Miledi, R. (1973) *J. Physiol. (London)* **231,** 549–574.
31. Hubbard, J. E. & Wilson, D. F. (1973) *J. Physiol. (London)* **228,** 307–325.
32. Negrete, J., Del Castillo, J., Escobar, I. & Yankelevich, G. (1972) *Nature New Biol.* **235,** 158–159.
33. Katz, B. & Miledi, R. (1965) *Proc. Roy. Soc. Ser. B* **161,** 483–495.
34. Feltz, A. & Mallart, A. (1971) *J. Physiol. (London)* **218,** 85–100.
35. Takeuchi, A. & Takeuchi, N. (1960) *J. Neurophysiol.* **23,** 397–402.
36. Gage, P. W. & Armstrong, C. M. (1968) *Nature* **218,** 363–365.
37. Anderson, C. R. & Stevens, C. F. (1973) *J. Physiol. (London)* **235,** 655–691.
38. Katz, B. & Miledi, R. (1972) *J. Physiol. (London)* **224,** 665–699.
39. Albuquerque, E. X., Barnard, E. A., Jansson, S.-E. & Wieckowski, J. (1973) *Life Sci.* **12,** 545–552.
40. Lebeda, F. J., Warnick, J. E. & Albuquerque, E. X. (1974) *Exp. Neurol.* **43,** 21–37.